

# SUCCESS RATES FOR INTEGRATED GPS AND GALILEO AMBIGUITY RESOLUTION

**Kees de Jong**

**Ezelsveldlaan 101, 2611 RV Delft, The Netherlands  
kdj101@hetnet.nl**

## ABSTRACT

Modernized GPS and the future European Galileo system will offer unprecedented accuracy and availability for precise positioning applications. For these applications, the ambiguities of the carrier observations have to be resolved to their integer values. The ambiguity success rate is a valuable design parameter to determine if the ambiguities can indeed be resolved correctly to their integer values. In this contribution, an overview is given of the modernized GPS and Galileo signals, followed by the models used for precise positioning over short, long and intermediate distances and the computation of ambiguity success rates. Finally, success rates are computed for a number of observation scenarios, ranging from current dual-frequency GPS to integrated triple-frequency GPS and Galileo.

**Keywords:** GPS, Galileo, ambiguity resolution, ambiguity success rate.

## RESUMO

A modernização do GPS e o futuro sistema Europeu denominado Galileo irão oferecer acurácia e disponibilidade nunca até então obtidas em aplicações de posicionamento de precisão. Para essas aplicações, as ambigüidades das observações de fase têm que ser resolvida como inteiras. A taxa de sucesso da solução da ambigüidade é um parâmetro que determina se as ambigüidades podem de fato ser solucionadas corretamente. Uma visão geral dos sinais GPS modernizado e do Galileo será apresentada neste artigo, seguida pelos modelos usados para posicionamento preciso de linhas bases com distâncias curtas, longas e intermediárias e do cálculo da razão do sucesso da ambigüidade. Finalmente, razões de sucesso são calculados para vários cenários de observações, desde o caso do GPS com dupla frequência até a frequência tripla do GPS e Galileo integrados.

**Palavras Chaves:** GPS, Galileo, solução da ambigüidade, razão de sucesso da ambigüidade.

### 1. INTRODUCTION

Precise positioning with Global Navigation Satellite Systems (GNSS), such as the US GPS and the future European Galileo, requires resolution of the ambiguities of the carrier phase observations to their integer values. The ambiguity success rate is defined as the probability of correctly fixing the ambiguities to their integer values. To compute the success rate, no actual data is required; it is therefore a valuable design parameter. In this contribution, the success rate will be used to evaluate the expected performance of modernized GPS and Galileo for a number of observation scenarios, which are a function of the number of satellite systems used, the number of frequencies and the length of the baseline vectors considered.

First a brief overview will be given of the modernized GPS and Galileo signals, followed by the measurement and stochastic models used to compute the

ambiguity success rates. Next, the success rates will be given for a number of observation scenarios, followed by conclusions.

### 2. MODERNIZED GPS

Between 1978 and 1985, 10 experimental so called GPS Block I satellites were launched. In 1989 the first operational Block II satellite was brought into orbit and the system reached full operational capability in 1994. Figure 1 gives an overview of the status of the current 28-satellite constellation. Although the constellation is performing well, a number of satellites are on single string, which means there is no redundancy to perform one or more critical tasks. Fortunately, for the period 2003-2006 13 new launches have already been scheduled to maintain constellation health, see Table 1.

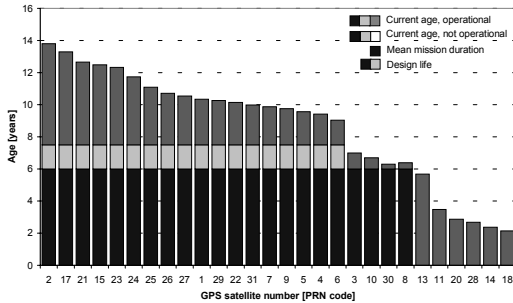


Figure 1 – GPS satellite configuration status (March 2003).

Table 1: GPS satellite launch schedule.

Year	Launches
2003	3 IIR
2004	2 IIR, 1 IIR-M
2005	3 IIR-M
2006	1 IIR-M, 1 IIF

Over the years, the mean mission duration (MMD) of the satellites has increased considerably. From a contractual MMD of six years and a design life of 7.5 years, the MMD has gone up to 9.6 years for the block II satellites to over 10 years for the block IIA satellites. For the latest block IIR and the new block IIR-M satellites, the design life is 10 years and the current MMD is nearly eight years. The future block IIF satellites, to be launched from 2006 onwards, will have a design life of 12 years and an MMD of 10 years. Originally these values were higher, but with the increased operational life span of the current satellites this would result in delaying further modernization into the completely redesigned GPSIII, which should provide users with the best possible satellite navigation system for the next 30 years.

Mass-market applications usually rely on tracking the C/A code on the L1 carrier (1575.42 MHz). For precision applications (cm accuracy or better), high-end dual-frequency receivers are in use. Over the years about 50,000 of these receivers have been sold. Before 1994 the P-code on the L2 carrier (1227.60 MHz) was freely available. After the encryption of the P-code into the secret Y-code, referred to as Anti-Spoofing (AS), manufacturers of civil receivers developed (semi-) codeless techniques to acquire and track the L2 signals anyway. However, a major drawback of the current approach to L2 signal recovery is that the special techniques that are required for it, due to the encryption of the P-code, results in a significant degradation of the signal to noise ratio. Unlike Selective Availability (SA), the intentional degradation of the GPS signals, which was discontinued in May 2002, AS will remain switched on.

The announcement of a second and third signal frequency therefore received a warm welcome from the civil GPS community. These signals will be modulated

on the current L2 frequency and the new L5 frequency of 1176.45 MHz.

The original plans aimed at a modulation of the L2-carrier with the same C/A-code as the L1-carrier. However, current GPS signals already date back to the 1970's and better alternatives are available. The European initiative to develop Galileo may have been another reason to look into a modernized GPS signal structure. Current discussions aim at developing and implementing a new civil GPS code, called L2 CS (for Civil Signal), see [USCG, 2003]. The new code should allow for signal tracking in adverse conditions when even the current L1 C/A-code signals can no longer be tracked, e.g., at low elevations or even inside buildings.

Details of the new signal can be found in [Fontana et al., 2001]. Compared with present semi-codeless techniques to get around Anti-Spoofing, measurement performance will improve considerably. Less cycle slips are to be experienced on L2 and satellites can be tracked further down to the horizon. Concerning measurement precision, a level similar to present L1 C/A-code performance is anticipated.

Eventually, the L2 CS-code might replace the L1 C/A-code in single-frequency mass-market applications. Dual-frequency range measurements are essential in high-precision applications to account for ionospheric delays and to enhance carrier phase ambiguity resolution. High-end civil dual-frequency systems will therefore be based on L1 C/A-code and L2 CS-code. It is not yet clear if the dual-frequency market will expand once the new L2 civil signal is available and if this, in addition, will give rise to price drops in receiver equipment.

GPS satellites that will transmit the new L2 signal will be launched from 2004 onwards. Full operational capability (FOC) is anticipated for 2012. By that time there will be about 28 satellites transmitting the new L2 signal.

The L5 signals will be transmitted by the Block IIF satellites, the first of which will be launched in 2006. The L5 signals will be different from the L2 CS, see again [USCG, 2003], and probably more similar to the current P-code, i.e., they will have a chipping rate that is 10 times that of the current C/A and the L2 CS codes. This high chipping rate code will offer high performance ranging capabilities as well as more robust carrier tracking for high-precision applications. It is anticipated that the L5 code measurement precision will be a few times better than the present L1 C/A-code precision, see [van Dierendonck and Hegarty, 2000]. Within 10 years, GPS will turn into a civil triple-frequency system. It is expected that high-end receivers, used for differential and relative positioning in precise geodetic and navigational applications, eventually will track code (pseudo range) and carrier phase on all three frequencies L1, L2 and L5, see Figure 2.

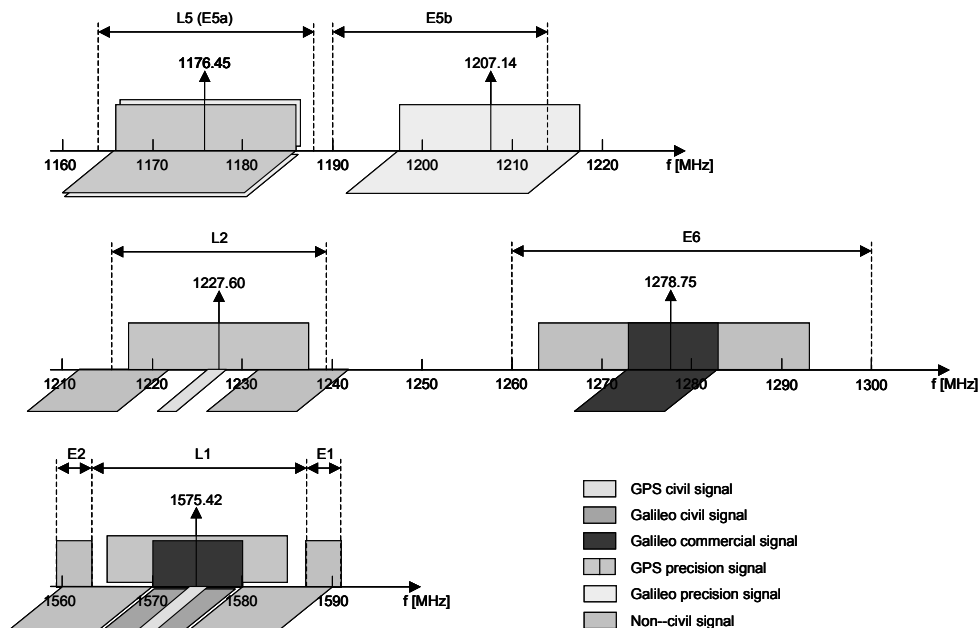


Figure 2 – GPS and Galileo signals.

The new GPS signals will affect both the space and user segment, i.e., both satellites and receivers. In addition, the GPS control segment will be modernized as well. New software will be installed to improve the quality of the GPS orbit and clock parameters, transmitted by the satellites in their navigation message. This will also be accomplished by extending the number of tracking stations. Finally, ephemeris and clock data will be uploaded to the satellites more frequently.

### 3. GALILEO

In March 2002, the European Commission gave the green light for the development of Galileo, the European counterpart of GPS. Galileo should be operational in 2008, when modernized GPS will have reached initial operational capability (IOC) with 18 satellites.

From a technical point of view, Galileo will be very similar to (modernized) GPS. According to [Salgado et al., 2001] the constellation will consist of 27 satellites, distributed evenly and regularly over three orbital planes. The constellation is probably enhanced by three active spare satellites. The projected altitude is slightly larger than for GPS. Table 2 gives an overview of the Galileo orbits.

Table 2: Galileo orbital parameters.

Orbital planes	3
Satellites/plane	9
Semi-major axis	29900 km
Inclination	56°
Eccentricity	~0

The frequency and signal plan of Galileo are not yet final. Since the frequency spectrum is extremely crowded, see e.g. [NTIA, 2003], only limited bandwidth is available. However, the proposal described in [Hein et al., 2001; Hein et al., 2002] is believed to serve as the current baseline. Like modernized GPS, Galileo will employ three bands in the frequency spectrum (see also Figure 2). Table 3 gives an overview of the frequency bands that may be used for Galileo.

Table 3: Galileo frequencies.

Identifier	Frequency
E2-L1-E1	1575.42 MHz
E5b	1207.14 MHz
E6	1278.75 MHz

At the upper end of the L-band spectrum, a small band is available on either side of the GPS L1-band. It is proposed to overlay the GPS L1 signal by using the very same center frequency of 1575.42 MHz. An overlay signal, with most power concentrated in the E2 and E1 side bands, is planned to be reserved for the so-called Public Regulated Service. An Open Service signal, also overlaid, would occupy a smaller band, in the GPS L1 signal band. See again Figure 2. Using special signal processing techniques, most of the power of the transmitted signal will be in the sidebands, to avoid interference with GPS L1. The resulting signal will provide pseudo-range measurements with a precision somewhere between that of GPS L1 C/A-code and future P-code.

At the lower end of the L-band spectrum, directly adjacent to the GPS L5-band, the E5-band has been reserved for Galileo. In the E5-band it is also possible to create an overlay with the GPS L5 signal. However, this band is wide enough to avoid this, if required. It is expected that the large bandwidth will result in a signal that has a performance comparable to the L5 GPS P-code. Due to the recent decision to shift the center frequency in the E5b-band from 1202.25 to 1207.14 MHz, some signal will be outside the E5-band.

Finally a reservation exists for Galileo in the mid-range of the L-band spectrum, as indicated in Figure 2. The E6-band is 40 MHz wide and is to be shared with radar applications. The signal in this band will be available for commercial services, as opposed to the other two signals, that are freely available (but remember that the current GPS L2 signal was also not meant for use by the civilian community). Measurement performance of the E6 signal will be comparable to that of E2-L1-E1.

More details on the proposed Galileo signals and frequencies are available from the Galileo website at <http://www.galileo-pgm.org>.

#### 4. PRECISE POSITIONING

Assuming measurements consist of code and carrier observations, collected at  $m$  different frequencies, the GNSS double-difference (DD) baseline measurement model for a single epoch  $k$  can be written as

$$\begin{pmatrix} p \\ \phi \end{pmatrix} = \begin{pmatrix} B & 0 \\ B & A \end{pmatrix} \begin{pmatrix} b \\ a \end{pmatrix} + \begin{pmatrix} C \\ -C \end{pmatrix} I \quad (1)$$

with  $p$  code observations,  $\phi$  carrier observations,  $b$  baseline parameters,  $a$  carrier ambiguities and  $I$  ionospheric effects. The corresponding covariance matrix reads

$$\begin{pmatrix} Q_p & 0 \\ 0 & Q_\phi \end{pmatrix} \quad (2)$$

There are several ways to deal with the ionosphere. In the ionosphere fixed model, we assume that ionospheric effects are absent. In that case, the parameters  $I$  are eliminated from (1). In the ionosphere float case, we assume the ionospheric effects are completely uncorrelated and unknown at both ends of the baseline.

The ionosphere fixed and float models are extreme cases. In many cases in practice baselines are too long to assume there are no residual ionospheric effects in the double difference data, but too short to assume these effects are completely unknown. We therefore introduce a third model, the ionosphere weighted model. For this model we extend the measurement model (1) with an additional vector of

ionospheric (pseudo-) observations,  $I_p$ , with covariance matrix  $Q_{I_p}$ . The measurement model becomes

$$\begin{pmatrix} p \\ \phi \\ I_p \end{pmatrix} = \begin{pmatrix} B & 0 \\ B & A \\ 0 & 0 \end{pmatrix} \begin{pmatrix} b \\ a \end{pmatrix} + \begin{pmatrix} C \\ -C \\ I \end{pmatrix} I \quad (3)$$

with covariance matrix

$$\begin{pmatrix} Q_p & 0 & 0 \\ 0 & Q_\phi & 0 \\ 0 & 0 & Q_{I_p} \end{pmatrix} \quad (4)$$

The weight of the ionospheric observations is governed by their standard deviations. For a standard deviation equal to zero, we arrive at the ionosphere fixed model, for a standard deviation approaching infinity, we obtain the ionosphere float model.

The parameters  $I_p$  can be eliminated from (3), resulting in a measurement model that has a similar structure as the ionosphere fixed model

$$\begin{pmatrix} p - CI_p \\ \phi + CI_p \end{pmatrix} = \begin{pmatrix} B & 0 \\ B & A \end{pmatrix} \begin{pmatrix} b \\ a \end{pmatrix} \quad (5)$$

and with covariance matrix

$$\begin{pmatrix} Q_p & 0 \\ 0 & Q_\phi \end{pmatrix} + \begin{pmatrix} -C \\ C \end{pmatrix} Q_{I_p} \begin{pmatrix} -C \\ C \end{pmatrix}^T \quad (6)$$

Note that (5) and (6) are completely equivalent to (3) and (4). In order to solve for the unknown parameters using least squares, we need the inverse of the covariance matrix of the observations. For the ionosphere float model, computing the inverse of (6) may be problematic. However, applying the matrix identity

$$(X + UYV)^{-1} = X^{-1} - X^{-1}U(Y^{-1} + VX^{-1}U)VX^{-1} \quad (7)$$

to (6) results in the inverse

$$\begin{pmatrix} Q_p^{-1} & 0 \\ 0 & Q_\phi^{-1} \end{pmatrix} - \begin{pmatrix} -Q_p^{-1}C \\ Q_\phi^{-1}C \end{pmatrix} D^{-1} \begin{pmatrix} -Q_p^{-1}C \\ Q_\phi^{-1}C \end{pmatrix}^T \quad (8)$$

where

$$D = Q_{I_p}^{-1} + C^T(Q_p^{-1} + Q_\phi^{-1})^{-1}C \quad (9)$$

For the ionosphere float model, the weights of the ionosphere observations become zero and we get

$$D = C^T (Q_p^{-1} + Q_\phi^{-1})^{-1} C \quad (10)$$

Note that for the ionosphere fixed model we can simply ignore the second term of (8).

Care should be taken to assign realistic weights to the ionospheric pseudo-observations. These observations may, e.g., be derived from the ionospheric estimates of permanent GPS arrays. In case no such information is available, one may have to revert to sample values of the ionospheric observations that are equal to zero. For this latter case the standard deviations of the ionospheric observations will be larger than for the former. The standard deviations should be chosen sufficiently large not to bias the estimated carrier ambiguities by an amount that may result in a wrong integer ambiguity. The effect of biases on integer carrier ambiguity resolution is described e.g. in [Teunissen, 2001].

If code and carrier observations are available, both baseline components and ambiguities can be resolved using only a single epoch of data (however, as we will see later, the probability of correctly solving the integer ambiguities may be very low). If only carrier observations are used, at least two epochs are required to solve for baseline components and ambiguities. The measurement model becomes

$$\begin{pmatrix} \phi_k + CI_{p,k} \\ \phi_j + CI_{p,j} \end{pmatrix} = \begin{pmatrix} B_k & 0 & A \\ 0 & B_j & A \end{pmatrix} \begin{pmatrix} b_k \\ b_j \\ a \end{pmatrix} \quad (11)$$

where the subscripts  $j$  and  $k$  denote the two epochs. Resolution of the integer ambiguities is only possible for the ionosphere fixed and weighted baselines; for the ionosphere float model, it is not possible to separate the ambiguities from the ionospheric effects.

Not using code observations has the advantage that effects due to multipath do not affect resolution of the integer ambiguities. However, there is also a disadvantage in that the number of satellites required to obtain a solution is much higher: four for a code and carrier solution, but seven for a carrier-only solution (for a moving receiver). This can be seen by eliminating the ambiguities from (11). What is left is a triple difference model with two different sets of position parameters at epochs  $j$  and  $k$ . There are six unknown

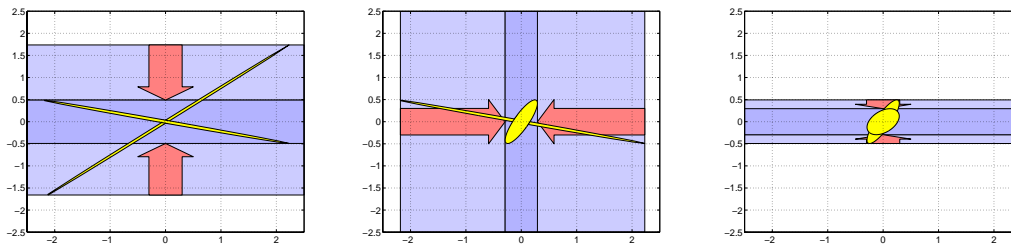


Figure 4 – Ambiguity decorrelation by pushing tangents. From left to right: 1) push horizontal tangents of confidence ellipse inwards; 2) push vertical tangents inwards; 3) repeat procedure until resulting ellipse resembles a circle as much as possible, i.e., until no further decorrelation of the ambiguities is possible. The areas of the original and decorrelated ellipse are the same and the integer nature of the ambiguities is preserved.

parameters; solving for these parameters requires six triple differences, which in turn require seven satellites.

If two different satellite systems are available, such as GPS and Galileo, the ambiguities of a mixed pair of double differences are in general not integer, due to different hardware and clock characteristics. Therefore the design matrix  $A$  and ambiguity vector  $a$  should be partitioned as

$$A = \begin{pmatrix} A_{GPS} & 0 \\ 0 & A_{Gal} \end{pmatrix} \quad a = \begin{pmatrix} a_{GPS} \\ a_{Gal} \end{pmatrix} \quad (12)$$

This also means that for a carrier-only GPS and Galileo solution, at least eight satellites are required.

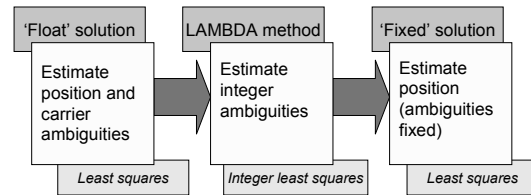
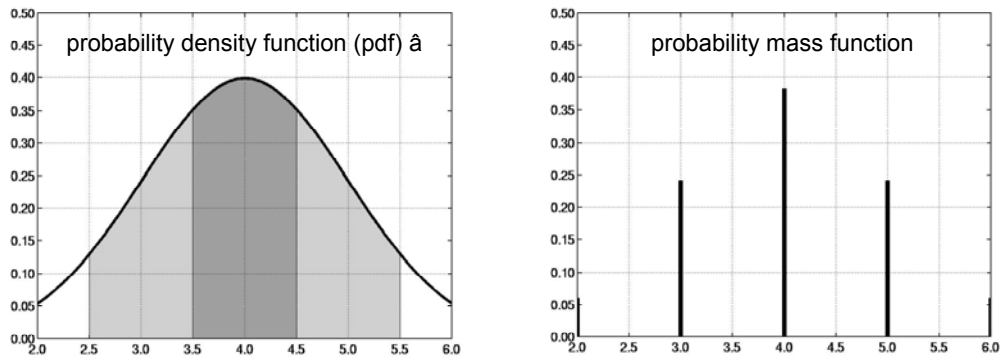


Figure 3 – The three steps involved in precise GNSS positioning.

## 5. AMBIGUITY RESOLUTION

Processing GPS data for precise relative positioning generally consists of the three steps shown in Figure 3. In the first step, known as the float solution, receiver positions, carrier ambiguities, and possibly a number of additional nuisance parameters, are determined in a least squares adjustment. The carrier ambiguities are known to be integers. However, after the first step, only real-valued ambiguities and their associated covariance matrix are available. These estimates and their covariance matrix are the input for the second step, in which the integer values of the carrier ambiguities are estimated. Once the integer ambiguities are known, they are applied to the carrier observations, after which these start acting as very precise pseudo range measurements. These adapted measurements are used as input for the third step, known as the fixed solution, in which the final, precise positions are determined.



$$\text{Success rate} = P(\tilde{a} = 4) = \int_{3.5}^{4.5} \text{pdf}(\hat{a})$$

Figure 5 – Computation of success rate, one-dimensional example (from [Teunissen & de Jong, 1999]).

The optimal method to resolve the ambiguities is based on integer least squares. An efficient implementation of this method for ambiguity resolution is the Least squares AMBiguity Decorrelation Adjustment (LAMBDA) method, developed at Delft University of Technology, [Teunissen, 1993], [de Jonge & Tiberius, 1996]. This method is based on a decorrelation of the original ambiguities, followed by a search procedure. The decorrelation is required since the spectrum of the conditional variances of the original ambiguities shows a large discontinuity. As a result, the search space will be very elongated and the search for the correct set of integer ambiguities will be very inefficient, [Teunissen et al., 1994]. After decorrelation of the ambiguities, the spectrum will be much more homogeneous, which results in a more efficient search procedure. A schematic overview of the decorrelation procedure is shown in Figure 4.

Denoting the real-valued ambiguities and their covariance matrix by  $\hat{a}$  and  $Q_{\hat{a}}$ , respectively, and the decorrelation matrix by  $Z^T$ , the transformed ambiguities and their corresponding covariance matrix are given by

$$\hat{z} = Z^T \hat{a} \quad Q_{\hat{z}} = Z^T Q_{\hat{a}} Z \quad (13)$$

The elements of the matrix  $Z^T$  are all integers; its determinant is equal to 1 or  $-1$ . After the integer values of the transformed ambiguities, denoted by  $\tilde{z}$ , are determined, the integer values of the original ambiguities are obtained by using the inverse of transformation (13)

$$\tilde{a} = Z^{-T} \tilde{z} \quad (14)$$

Contrary to popular belief, the resolved carrier ambiguities are stochastic rather than deterministic. The integer ambiguities are determined from observations and since these observations carry an inherent uncertainty, the integer ambiguities are also subject to

this uncertainty. Rather than stating that the ambiguities are determined from the observation data, it is more appropriate to say that they are *estimated* from this data.

The ambiguities being estimated have an important implication: they may not always be correct. What we would like to know is, given a particular estimate, the probability that this estimate is indeed the correct integer or integer vector. This probability of correct integer ambiguity estimation will be referred to as success rate, [Teunissen, 1998]. For the computation of the success rate, we need the probability mass function of the integer least squares estimator. This probability mass function can be constructed from the probability density function of the real-valued ambiguity estimates resulting from the float solution, and the integer mapping applied in the second step. The characteristics of the probability density function are captured in the covariance matrix of the real-valued ambiguities. This covariance matrix is a function of the a priori stochastic model of the observations and of the relative receiver-satellite geometry. For its computation no actual data is required. Consequently, for the computation of success rates, also no observation data is required. As such, it can be used as a design tool, just like the popular DOP (Dilution of Precision) values.

Another application of the success rate is its use as a system design parameter when looking for the best possible combination of frequencies for integer ambiguity estimation. Examples of the success rate as a planning and design tool will be given in Section 6.

To illustrate the computation of success rates, we will consider a simple, one-dimensional example. The probability density function of the real-valued estimator is shown in Figure 5. This function is continuous because the real-valued estimator can take any real value. The function is centered at the correct integer, due to the unbiasedness of the least squares estimator.

For this case, we assume that the correct integer ambiguity is equal to four. In one dimension,

integer estimation boils down to simple rounding. All real-valued estimates in an interval of +0.5 and -0.5 around an integer value are mapped onto that integer. The probability that the integer least squares estimator takes on a particular integer value can therefore be computed by integrating the probability density function of the real-valued estimator over these mapping intervals. Consequently, the success rate is equal to the integral of the probability density function over the mapping interval around four, see again Figure 5.

Denoting the probability of correctly resolving the decorrelated integer ambiguities by  $P(\tilde{z} = z)$ , a lower bound of the probability of correct integer ambiguity resolution, i.e., the success rate, is given by

$$P(\tilde{z} = z) \geq \prod_{i=1}^n \left( 2\Phi\left(\frac{1}{2\sigma_{\tilde{z}_{i|I}}}\right) - 1 \right) \quad (15)$$

where  $n$  is the number of ambiguities,  $\sigma_{\tilde{z}_{i|I}}^2$  is the conditional variance, resulting from the decomposition  $Q_{\tilde{z}} = LDL^T$  of the covariance matrix of the transformed ambiguities, with  $L$  a lower triangular matrix,  $D$  a diagonal matrix and  $\sigma_{\tilde{z}_{i|I}}^2 = D(i, i)$ . The function  $\Phi$  is defined as

$$\Phi(x) = \int_{-\infty}^x \frac{1}{\sqrt{2\pi}} \exp\left(-\frac{1}{2}z^2\right) dz \quad (16)$$

which is the integral of the Gaussian probability density function.

## 6. SUCCESS RATES

Success rates were computed for São Paulo (latitude 23°32' S, longitude 46°37' W), for 23 March 2003, using a minimum elevation of 10°. Standard deviations of the undifferenced carrier observations were 0.003 m, the standard deviations of the code observations are given in Table 4. As explained in Sections 2 and 3, the precision of the code observations depend on the signals considered for both GPS and Galileo. Unless indicated otherwise, the a priori standard deviation of single-difference ionospheric pseudo-observations was chosen as 0.05 m, corresponding to a baseline length of about 50 km.

Table 4: Standard deviations of code observations, used for computation of success rates.

Standard precision			
L1	0.30	E2-L1-E1	0.15
L2	0.30	E5b	0.10
L5	0.10	E6	0.10
High precision			
L1	0.30	E2-L1-E1	0.10
L5	0.05	E5b	0.05

Success rates are computed for a number of scenarios. For the first three scenarios, ionosphere fixed (short baselines), ionosphere weighted (medium baselines) and ionosphere float (long baselines) will be considered for single-epoch ambiguity resolution. These scenarios include:

1. GPS-only, dual- and triple-frequency.
  2. Integrated GPS and Galileo, dual- and triple-frequency.
  3. Integrated GPS and Galileo, dual-frequency, different standard deviations of code observations.
- For the fourth scenario, only the weighted ionosphere model will be considered. Rather than looking at single-epoch success rates, the number of epochs required to obtain a predefined success rate of 99% are computed:
4. Integrated GPS and Galileo, dual-frequency, success rate of 99%, different standard deviations of code observations and different standard deviations of ionospheric pseudo-observations.

The results are shown as 95% percentiles, which mean that in 95% of all cases (during the day considered), the success rate is greater than the indicated value.

Shown in Figure 6 are the number of visible GPS and Galileo satellites for São Paulo on 23 March 2003. Visible here means above the cut-off elevation of 10°. As we can see, the total number of satellites ranges from 12 to 21. It should be noted here that, unlike GPS, the Galileo constellation does not repeat itself every sidereal day (23h56m) but every five days. As a result, the number of satellites, and the results given later in this section, will vary from day to day.

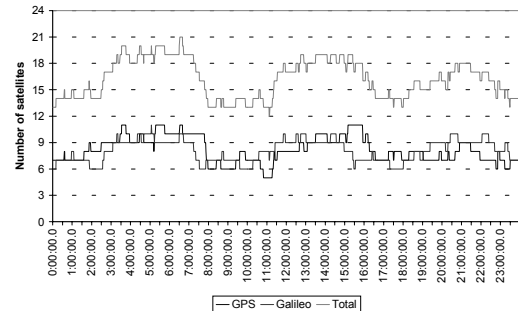


Figure 6 – Number of visible satellites (above 10° elevation mask) for São Paulo, 23 March 2003.

Shown in Figure 7 are the success rates for the GPS-only cases. The dual-frequency results are based on the current L1 and L2 frequencies, for the triple-frequency results the new L5 signal was added. For short baselines, the dual-frequency success rates are already very high, so adding a third frequency has only a marginal effect. The situation is different for the medium and long baseline cases, although it can be concluded that instantaneous ambiguity resolution is not feasible for most of the time.

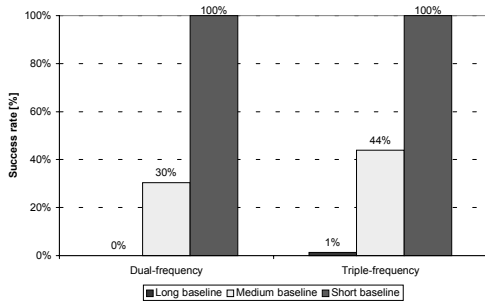


Figure 7 – Instantaneous success rates for the GPS-only case (standard precision of code observations).

For an integrated GPS/Galileo solution, the success rates show a significant improvement, compared to the GPS-only case (see Figure 8). In particular for the weighted ionosphere model (medium baseline length) instantaneous ambiguity resolution becomes feasible during most of the day. The dual-frequency Galileo system considered here was assumed to use the E2-L1-E1 frequency of 1575.42 MHz and the E5b frequency of 1207.14 MHz.

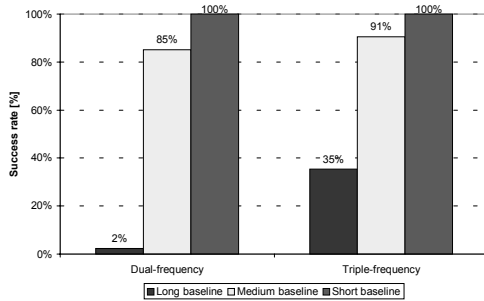


Figure 8 – Instantaneous success rates for integrated GPS/Galileo positioning (standard precision code observations).

In the third scenario, only dual-frequency GPS (L1, L5) and Galileo (E2-L1-E1, E5b) were considered for different precisions of the code observations, see Table 4. As can be seen from Figure 9, the long baseline (ionosphere float model) benefited the most from the improved precision of the code observations. High precision code observations are even more beneficial than standard precision observations for the triple-frequency case. However, instantaneous ambiguity resolution is possible for only a limited period of the day.

For the last scenario again the integrated dual-frequency GPS and Galileo system from scenario 3 were considered, but this time only for the medium baseline case. Instead of looking at single-epoch ambiguity resolution, it was now investigated how many epochs were required for a success rate of 99%. Results are shown in Figure 10 for the standard- and high-precision code measurements for a standard deviation of 0.05 m for the ionospheric pseudo-observations; in the same figure similar results are shown for a standard deviation of 0.10 m for these pseudo-observations. It can be concluded that only a limited (2-4) number of

epochs are required to attain a success rate of 99%. A second conclusion is that improved code observations do not contribute much to reducing the number of epochs required to attain a predefined success rate. Formulated differently, code observations do not contribute much when processing more than one epoch.

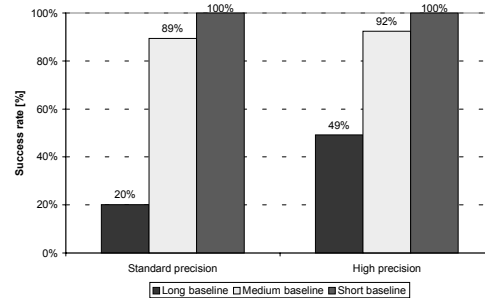


Figure 9 – Instantaneous success-rates for integrated dual-frequency GPS/Galileo and different precisions for the code observations (see Table 4).

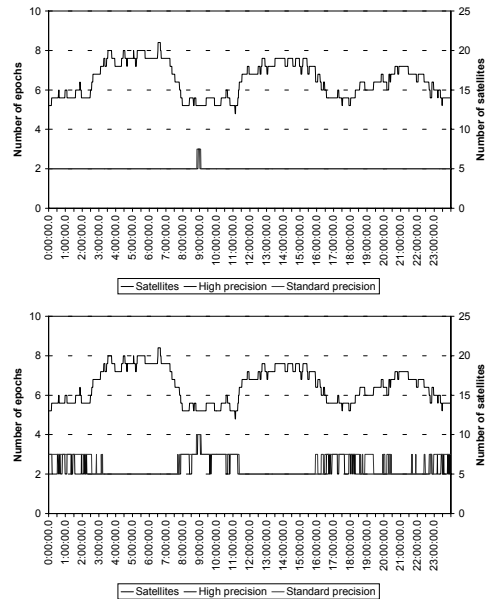


Figure 10 – Number of epochs, required to attain a success rate of 99% for dual-frequency GPS/Galileo and standard and high precision code observations and for an ionospheric pseudo-observations standard deviation of 0.05 m (top) and 0.10 m.

The carrier observations in this case seem to provide enough geometrical strength by themselves to warrant reliable ambiguity resolution. The additional advantage is that it is not necessary to use code observations, which often suffer from multipath, which in turn affect the resolution of the carrier ambiguities, see [Joosten et al., 2002].



## 7. CONCLUSIONS

For integrated GPS/Galileo positioning ambiguity success rates are significantly higher than for GPS-only, in particular for medium and long baselines. However, for very long baselines, instantaneous ambiguity resolution is not feasible, due to ionospheric effects. Fortunately, the influence of the ionosphere is smaller for shorter baselines. For medium baselines (up to 100 km), ambiguities can be resolved nearly instantaneously, using only a limited number of observation epochs.

## 8. REFERENCES

- FONTANA, R.D., W. CHEUNG, P.M. NOVAK, T.A. STANSELL, JR., 2001. The new L2 civil signal. **Proceedings ION GPS 2001**, Salt Lake City, USA, pp. 617-631.
- HEIN, G.W., J. GODET, J.L. ISSLER, J.C. MARTIN, R. LUCAS-RODRIGUEZ, T. PRATT, 2001. The Galileo frequency structure and signal design. **Proceedings ION GPS 2001**, Salt Lake City, USA, pp. 1273-1282.
- HEIN, G.W., J. GODET, J.L. ISSLER, J.C. MARTIN, P. ERHARD, R. LUCAS-RODRIGUEZ, T. PRATT, 2001. Status of Galileo frequency and signal design. **Proceedings ION GPS 2002**, Portland, USA, pp. 266-277.
- DE JONGE, P., C. TIBERIUS, 1996. **The LAMBDA method for integer ambiguity estimation: implementation aspects**. Delft Geodetic Computing Centre, LGR series No. 12, Delft University of Technology, Delft, v+49 pp.
- VAN DIERENDONCK, E.J., C. HEGARTY, 2000. The new L5 civil GPS signal. **GPS World**, Vol. 11, No. 9, pp. 64-71.
- JOOSTEN, P., T. PANY, J. WINKEL, 2002. The impact of unmodelled multipath on ambiguity resolution. In: **Proceedings ION GPS 2002**, Portland, USA, pp. 953-961.
- NTIA, 2003. US frequency allocation chart. <http://www.ntia.doc.gov/osmhome/allochrt.html> (accessed 23 March 2003).
- SALGADO, S., S. ABBONDANZA, R. BLONDEL, S. LANNELONGUE, 2001. Constellation availability concepts for Galileo. **Proceedings ION NTM 2001**, Long Beach, USA, pp. 778-786.
- TEUNISSEN, P.J.G., 1993. **Least-squares estimation of the integer GPS ambiguities**. Invited lecture, Section IV Theory and Methodology, IAG General Meeting, Beijing; also in Delft Geodetic Computing Centre, LGR series No. 6, Delft University of Technology, Delft, 16 pp.
- TEUNISSEN, P.J.G., 1998. Success probability of integer GPS ambiguity rounding and bootstrapping. **Journal of Geodesy**, 72, pp. 606-612.
- TEUNISSEN, P.J.G., 2001. Integer estimation in the presence of biases. **Journal of Geodesy**, 75, pp. 399-407.
- TEUNISSEN, P.J.G., P.J. DE JONGE, C.C.J.M. TIBERIUS, 1994. On the spectrum of GPS DD ambiguities. **Proceedings ION GPS-94**, Salt Lake City, USA, pp. 115-124.
- TEUNISSEN, P.J.G., C.D. DE JONG, 1999. Predicting the success of ambiguity resolution. Presented at 34<sup>th</sup> CGSIC meeting, Nashville, USA. <http://www.-navcen.uscg.gov/cgsic/default.htm> (accessed 23 March 2003).